# Turbulent Heat Flux Model for Shock-Boundary Layer Interaction with Non-Adiabatic Wall

**By Subhajit Roy † AND Krishnendu Sinha ‡**

Department of Aerospace Engineering, Indian Institute of Technology Bombay, India

The interaction between shock wave and turbulent boundary layer (STBLI) can enhance the thermal load on the vehicle surface dramatically in high-speed flows. Reynolds-averaged Navier-Stokes simulations based on constant turbulent Prandtl number often give grossly erroneous heat transfer predictions in STBLI flows. This is due to the fact that the underlying Morkovin's hypothesis breaks down in the presence of shock waves and highly cooled walls. In this work, we develop a turbulent heat flux model for non-adiabatic walls based on the shock-turbulence interaction physics and boundary layer direct numerical simulation (DNS) data. This is an extension of our earlier work. The model is combined with the well-validated shock-unsteadiness $k$-$\omega$ model and is used to study two cone-flare cases involving shock/boundary-layer interactions at hypersonic Mach numbers and high Reynolds number. Comparison with experimental data shows significant improvement in the surface heat transfer rate in the interaction region.

## 1. Introduction

The next generation of high-speed vehicles will travel through the atmosphere at hypersonic speeds . Efficient design of hypersonic vehicles, including the prediction of skin friction and surface heat transfer, requires good understanding of the hypersonic turbulent boundary layer and shock waves. The interaction of shock waves and turbulent boundary layer is very common in high-speed flows and is responsible for high aero-thermal load on the vehicle.

Most of our current understanding of shock wave turbulent boundary layers interaction (STBLI) is based on the results of supersonic Mach numbers (M < 5) . There are very few works available in the literature which deal with hypersonic turbulent boundary layer and its interaction with the shock waves. One of the major difference between supersonic and hypersonic boundary layers is the wall temperature condition. At supersonic speeds, the surface temperature is essentially adiabatic; while at hypersonic speeds, due to considerable radiative cooling and internal heat transfer or due to necessary wall cooling to prevent melting, the surface temperatures are significantly lower than the adiabatic wall temperature. As a result, the conductive heat transfer between the boundary layer flow and the surface of hypersonic vehicles is enormous.

Predicting turbulent heat transfer in high-speed flows dominated by shock waves poses significant challenge to computational fluid dynamics (CFD) methods [1, 2]. The majority of the turbulence models are based on the gradient diffusion hypothesis, where the turbulent heat flux is modeled in terms of turbulent conductivity and turbulent Prandtl

† Graduate student
‡ Professor

number ($Pr_T$). Conventional turbulence models in Reynolds-averaged Navier-Stokes (RANS) simulations use a constant $Pr_T$ value of 0.89; they often overpredict the wall heat transfer in STBLI flows. A few variable $Pr_T$ models proposed in literature improve the heat flux prediction, but are computationally intensive [3, 4].

In a recent work, Roy *et al.* [5] study the interaction of turbulent fluctuations with a normal shock to propose a new model for the turbulent heat flux. The unsteady oscillations of an otherwise steady (in the mean) shock wave are found to have a dominant effect. It is modeled using the shock-unsteadiness model of Sinha *et al.* [6], which is based on linear interaction analysis of shock-turbulence interaction. The model is found to match direct numerical simulation (DNS) data for the peak turbulent heat flux generated by shock waves [7]. Roy *et al.* [5] cast the physics based turbulent heat flux model in a variable $Pr_T$ form, so as readily integrate it into existing CFD codes. As per the new model, the turbulent Prandtl number is a function of the shock strength and the shock-unsteadiness parameter. It takes a value lower than the conventionally accepted value of 0.89 and the value decreases for stronger shock waves. A lower $Pr_T$ results in a higher turbulent conductivity and a higher turbulent heat flux than conventional models. More heat convected away from the wall by fluid turbulence leads to a lower peak heat transfer to the wall. The results match the peak heating measured in oblique shock boundary layer interaction for a range of shock strengths at Mach 5 [8].

A limitation of the proposed model is that it is uses Morkovin's hypothesis [9] for the boundary layers upstream of the shock. This may not work in the presence of severe wall cooling or heating, which is measured in terms of the ratio of the wall temperature to the recovery temperature (defined as $T_r = T_\infty[1 + r_c\frac{\gamma-1}{2}M_\infty^2]$). Shock-boundary layer interaction occurring at hypersonic flight conditions usually correspond to highly cooled walls (as mentioned above). Even ground-based experimentation, for example, over flat plates at 300 K can give $T_w/T_r$ = 0.1 for Mach numbers in the range 7–8. Experiments over heated and cooled plates have found substantial enhancement and/or reduction of the separation bubble in the interaction region [10, 11]. Similar results are also reported in direct numerical simulation, where the wall to recovery temperature is varied systematically for SBLI at supersonic Mach numbers [12, 13]. Recently, large eddy simulation is employed to explore SBLI at hypersonic Mach numbers and to design experiments involving heated/cooled walls in the HEG tunnel in DLR, Göttingen [14]. In short, there is a surge of recent interest in the study of SBLI over non-adiabatic walls, both in terms of the physics and it's potential in the control of the SBLI phenomenon. Simulating these effects accurately is an inherent part of the research effort, as the highest heating loads are reported for SBLI over highly cooled walls [12].

In this work, we extend the earlier variable $Pr_T$ model to study the effect of non-adiabatic wall on shock-boundary layer interaction in the Reynolds-average Navier-Stokes framework. We employ linear interaction analysis and DNS data [15, 16] to estimate the turbulent heat flux generated by shock waves which is finally cast in turbulent Prandtl number form and is sensitive to wall heating and cooling. The results are compared with the available experimental data.

## 2. Methodology

We solve the axisymmetric Reynolds-averaged Navier-Stokes equations presented by Wilcox [17] for the mean flow. The two-equation $k$-$\omega$ model of Wilcox (refered to as baseline model here) and the recent shock-unsteadiness corrected $k$-$\omega$ model of Veera

and Sinha [18] are used in the simulations. Both the baseline and shock-unsteadiness corrected $k$-$\omega$ models do not include any compressibility corrections„ as they are found to deteriorate model predictions in the undisturbed boundary layer upstream of the interaction [19, 20]. Compressibility corrections of the form of dilatational dissipation reduce the turbulent kinetic energy in the boundary layer, and thus decrease the skin friction coefficient compared to well-established correlations for zero pressure-gradient turbulent boundary layers.

The governing equations are discretised in a finite volume formulation, where the inviscid fluxes are computed using a modified, low-dissipation form of the Steger-Warming flux splitting approach [21]. This method reduces the numerical dissipation, and is found to be useful for high-speed flows with strong shock waves and viscous-inviscid interactions with boundary layers. As a result, very thin and well-defined shock waves are captured over a few grid cells. The turbulence model equations are fully coupled to the mean flow equations. The details of the formulation are given by Sinha and Candler [22]. The method is second-order accurate in space. The viscous fluxes and the turbulent source terms are evaluated using second-order accurate central difference method. The implicit Data Parallel Line Relaxation method of Wright *et al.* [23] is used to integrate in time and reach steady-state solution.

At the wall, isothermal temperature and no-slip boundary conditions are applied, and extrapolation condition is used at the exit boundary of the domain for all the simulations. A supersonic boundary condition is imposed at the top boundary of the domain. For the turbulence quantities, the boundary conditions at the wall [24] are taken as $k$ = 0 and $\omega = 60\nu_w/\beta_1\Delta y_1^2$, where $\nu_w$ is kinematic viscosity at the wall, $\beta_1$ = 3/40 and $\Delta y_1$ is the normal distance to the grid point nearest to the wall. Following Menter [24], the free stream conditions used for all the simulations are $\omega_\infty = 10U_\infty/L$ and $k_\infty = 0.01\nu_\infty\omega_\infty$ where L = 2.35 m (horizonal length of the cone) is the characteristic length of the geometry.

### 2.1. *Model development*

The current heat flux model for non-adiabatic wall builds upon the variable $Pr_T$ model presented by Roy *et al.* [5] and Roy and Sinha [25, 26]. The use of Walz' relation [27] makes the model implementation much simpler and robust than the earlier versions of the model.

Generally, the turbulent heat flux vector $q_{T,j}$ is modeled using the gradient diffusion hypothesis

$$q_{T,j} = -\kappa_T \frac{\partial \overline{T}}{\partial x_j}, \tag{2.1}$$

where $\kappa_T$ is the turbulent conductivity of heat. It is related to eddy viscosity via the turbulent Prandtl number $Pr_T$ and the specific heat of the gas at constant pressure $c_p$.

$$\kappa_T = \frac{\mu_T c_p}{Pr_T} \tag{2.2}$$

Morkovin hypothesis [9] relates the turbulent heat flux to the Reynolds stress in a compressible turbulent boundary layer and thus prescribes a constant value of the turbulent Prandtl number. However, the assumption of zero total temperature fluctuation in Morkovin's hypothesis is not valid across a shock wave and highly cooled turbulent boundary layer. The applicability of Morkovin's hypothesis has been called into question by several researcher in last decade. Leschziner [28] and Duan [16] suggest that

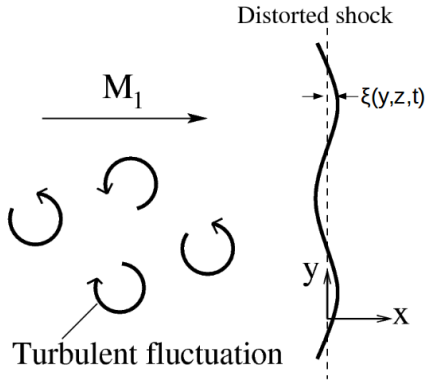


FIGURE 1. Schematic of a distorted shock wave while interacting with the upstream turbulence.

the amount of total temperature fluctuations $T_0'$ can be neglected up to a moderate Mach number 3 and wall cooling ratio $T_w/T_r$ 0.5. As per the work of Duan *et al.* [16], the rms value of $T_0'$ is close to 25% of mean total temperature for a Mach 5 turbulent boundary layer with $T_w/T_r$ equal to 0.18.

The work of Xiao *et al.* [3] and others show that a variation of turbulent Prandtl number improves the heat flux prediction capabilities of standard turbulence models significantly. We use the conservation of total enthalpy to model the shock-normal turbulent heat flux behind the shock wave. The shock wave undergoes unsteady motion in response to the fluctuations in a turbulent flow, see Fig. 1. The deviation of the shock from its mean position is taken as $\xi(y,z,t)$, such that the temporal derivative $\xi_t$ represents the instantaneous shock speed in the streamwise direction. The total temperature in the shock reference frame is written as

$$T_0 = \overline{T} + T' + \frac{\left(\overline{u} + u' - \xi_t\right)^2 + v'^2 + w'^2}{2c_p}. \tag{2.3}$$

Here, $u$,$v$,$w$ are the velocity components, overbar represents mean flow quantity and primes denote turbulent fluctuations. Assuming the shock speed and fluctuations to be small as compared to the jumps in the mean flow quantities across the shock, the linearized total temperature conservation across the shock is given as:

$$T_1' + \frac{\overline{u_1}u_1'}{c_p} = T_2' + \frac{\overline{u_2}u_2'}{c_p} + \frac{\xi_t}{c_p}(\overline{u_1} - \overline{u_2}), \tag{2.4}$$

where 1 and 2 denote the shock upstream and downstream location respectively. The left-hand side of the above equation represents the upstream total temperature fluctuations whereas the first two terms in the right hand side denote the downstream total temperature fluctuation and the last term in the right hand side corresponds to the unsteady shock oscillation.

The level of upstream total temperature fluctuations in a boundary-layer is not readily available in RANS simulations for non-adiabatic walls. We follow the work of Huang *et al.* [29] to find a relation between upstream velocity and temperature fluctuations. The modified strong Reynolds analogy of Huang , also known as Huang's strong Reynolds analogy (HSRA), is based on the the mixing length assumption and it is found to match the DNS data well compared to any other form of the strong Reynolds analogy (SRA).

As per HSRA the velocity-temperature fluctuations in a compressible turbulent boundary layer is given as

$$A_{uT} = -\frac{T'/\overline{T}}{u'/\overline{u}} = (\gamma-1)M^2 \frac{1}{Pr_T}\left(\frac{\partial \overline{T_0}}{\partial \overline{T}} - 1\right)^{-1}. \tag{2.5}$$

We denote the left hand side of the above equation as $A_{uT}$ for simplicity. Roy and Sinha [25] use the local flow variables to compute temperature derivative in a CFD simulation and thus compute $A_{uT}$. In this work, we use Walz' temperature distribution [27] for zero pressure-gradient turbulent boundary layer to calculate the temperature derivative and the $A_{uT}$ expression becomes

$$A_{uT} = (\gamma-1)M^2\left(1 - \frac{u_\infty}{2\overline{u}}\left[\frac{1-\dfrac{T_w}{T_r}}{1-\dfrac{T_\infty}{T_r}}\right]\right). \tag{2.6}$$

Note that the above expression will get back to the Morkovin's hypothesis for adiabatic wall ($T_w/T_r = 1$). We use the above expression of $A_{uT}$ in the left hand side of Eq. 2.4 to get

$$-A_{uT}u_1'\frac{\overline{T_1}}{\overline{u_1}} + \frac{\overline{u_1}u_1'}{c_p} = T_2' + \frac{\overline{u_2}u_2'}{c_p} + \frac{\xi_t}{c_p}(\overline{u_1} - \overline{u_2}) \tag{2.7}$$

On taking a moment with $u_2'$, we get

$$\overline{u_2'T_2'} = -\frac{\overline{u_2}}{c_p}\left(\overline{u_2'^2} + \overline{u_2'\xi_t}(r-1) - r\overline{u_1'u_2'} + A_{uT}c_p\frac{\overline{T_1}}{\overline{u_2}\,\overline{u_1}}\overline{u_1'u_2'}\right), \tag{2.8}$$

where $r$ is the mean density ratio across the shock wave. The unclosed correlation $\overline{u'\xi_t}$ is modeled as per the shock-unsteadiness model of Sinha *et al.* [6] and its computationally robust form given by Roy *et al.* [5]

$$\overline{u'\xi_t} = b_1\overline{u'^2} \quad \text{with} \quad b_1 = 0.4 + 0.2A_{uT} + 0.6\left(\frac{6-r}{5}\right)^{5.2}. \tag{2.9}$$

The above equation is based on the assumption that the unsteady shock motion is caused by the incoming turbulent velocity fluctuations, and the closure coefficient $b_1$ is obtained from linear interaction analysis. The aforementioned model accounts only the shock motion at frequencies comparable to that of the incoming turbulence. Additional low-frequency shock oscillations, observed in the SBLI, have a negligible correlation with the turbulent velocity fluctuations in the boundary layer. Such low frequency shock motion do not contribute to the $\overline{u'\xi_t}$ correlation. We thus get the downstream shock normal heat flux as

$$\overline{u'T'} = -\frac{\overline{u}}{c_p}\overline{u'^2}\left(1 + b_1(r-1) - \beta\right), \tag{2.10}$$

where $\beta = \alpha r(1 - A_{uT}/(\gamma-1)M_1^2)$ and $\alpha = \dfrac{\overline{u_1'u_2'}}{\overline{u_2'^2}} = 0.6 + 0.4\left(\dfrac{6-r}{5}\right)^{5.2}$. The equivalent

turbulent Prandtl number is given as

$$Pr_T = \frac{3}{4}\left(\frac{1}{1+b_1(r-1)-\beta}\right), \tag{2.11}$$

where the shock-normal Reynolds stress is modeled in terms of the Boussinesq approximation .

The above expression of $Pr_T$ is very similar to that of Roy and Sinha [25] except the $\beta$ term which combined the effect of upstream velocity and temperature fluctuations here. Also the $A_{uT}$ expression is calculated using Huang's strong Reynolds analogy and Walz's equation to incorporate the wall cooling effect.

### 2.2. *Shock function formulation*

Roy *et al.* [5] composed a transport equation for a scalar shock function $\psi$ to evaluate the mean density ratio at the shock region. The turbulent Prandtl number is then modeled in terms of $\psi$. The transport equation for $\psi$ is such that it deviates from its undisturbed value $\psi_0$ only in the regions of strong compression and gradually relaxes back from the shock value to the reference value.

$$\frac{\partial(\overline{\rho}\psi)}{\partial t} + \frac{\partial(\overline{\rho}\widetilde{u_i}\psi)}{\partial x_i} = \overline{\rho}\psi S_{ii} - \overline{\rho}(\psi-\psi_0)\frac{\sqrt{\widetilde{u_i}\widetilde{u_i}}}{L_\epsilon}, \tag{2.12}$$

where $S_{ii} = \frac{\partial \widetilde{u_i}}{\partial x_i}$ is the mean dilatation, $\sqrt{\widetilde{u_i}\widetilde{u_i}}$ is the mean velocity magnitude and $L_\epsilon = \sqrt{k}/\omega$ is the dissipation length scale in the $k$-$\omega$ framework. Integrating the differential equation across a shock gives the shock value $\psi_s$ as

$$\frac{\psi_s}{\psi_0} = \frac{\overline{u_2}}{\overline{u_1}} = \frac{1}{r} \tag{2.13}$$

Thus, $\psi_s$ is an indicator of the shock strength and an upstream undisturbed value of $\psi_0 = 1$ ensures that we get $\psi_s = 1/r$ at the shock location.

Substitution of $r = 1/\psi$ in Eq. (2.11) gives an expression for turbulent Prandtl number as

$$Pr_T = \frac{3/4\zeta}{1+b_1(\psi^{-1}-1)-\beta} \tag{2.14}$$

where an additional factor $\zeta$ is introduced to make the formulation consistent with the conventionally accepted $Pr_T$ value of 0.89 in boundary layers without shock waves. For vanishing shock strength in the limit $M_1 \to 1$, r $\to$ 1 and $\psi \to 1$ , $Pr_T$ should take a value of 0.89. Thus, $\zeta$ is defined as

$$\zeta = 1 + \left(\frac{0.89}{0.75}(1-\beta) - 1\right) exp\left(\chi(1-\frac{1}{\psi})\right). \tag{2.15}$$

such that it approaches 1 in the presence of shock waves. Here $\chi$ is model parameter and its value is equal to 1000; see Roy *et al.* [5] for more details.

## 3. Results

We consider the axisymmetric cone-flare configurations of Holden *et al.* [30] and the test conditions are listed in table 1. The geometry consists of a 2.5 m long (horizontal length) 7° half-angle cone and a 40° flare, which gives a 33° turning angle at the cone-flare junction. The computational domain extends from the tip of the cone to the end of

| | Deflection angle | $M_\infty$ | $\rho_\infty$ (kg/m$^3$) | $T_\infty$ (K) | $T_w$ (K) | $Re_\infty$/m $\times 10^6$ | $T_w/T_r$ | $H_0$ (MJ/kg) | $k_\infty, 10^{-3}$ (m$^2$s$^{-2}$) | $\omega_\infty, 10^4$ (s$^{-1}$) |
|---|---|---|---|---|---|---|---|---|---|---|
| Cone- | 33° | 8.21 | 0.0437 | 60.4 | 306.5 | 14.30 | 0.38 | 0.87 | 5.00 | 0.54 |
| flare | 33° | 7.18 | 0.0572 | 66.6 | 302.5 | 15.60 | 0.44 | 0.76 | 3.90 | 0.50 |

TABLE 1. The freestream and wall conditions in the SBLI experiments [30].

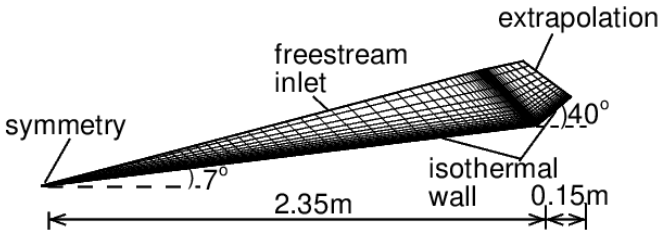


FIGURE 2. Computational mesh with boundary conditions showing every third point in each direction.

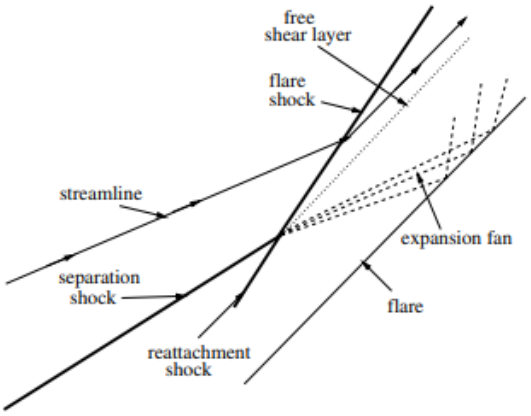


FIGURE 3. Schematic sketch of Edney type VI shock–shock interaction [31].

the flare, and the outer boundary is tailored to the inviscid cone shock. The computational grid consists of 450×150 points, with fine grid at the cone tip and the cone-flare junction; see Fig. 2. Refining the grid to 850×250 points shows minimal changes in the solution, within 1.5% in the flare heat flux prediction for the strongest interaction at Mach 8.21. The first point next to the wall is placed at $10^{-6}$ m, which is equivalent to 0.5 wall units or less along the cone-flare surface. A small symmetry plane is added in front of the cone tip to avoid a stagnation point boundary condition.

The flow topology for Mach 8.21 case is similar to that presented in [31], where an intersection of the separation shock with the reattachment shock results in a type VI shock-shock interaction. Expansion waves and high entropy shear-layer are emanated

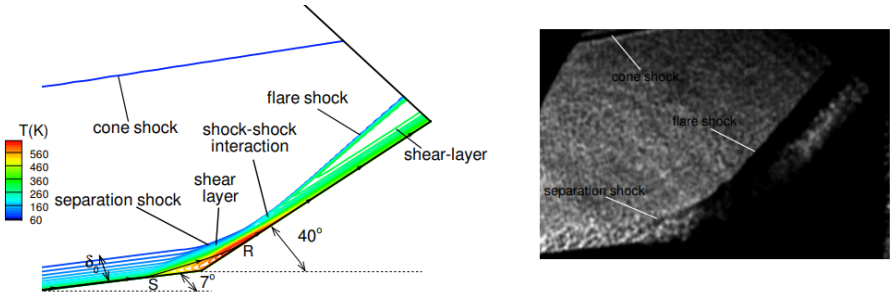


FIGURE 4. Comparison of computed temperature contours, using (a) shock unsteadiness $k$-$\omega$ model, and (b) experimental schlieren image [30] for $M_\infty = 8.21$ case.

at the shock-shock interaction point; see Fig. 3 for further details. The computed temperature contours for Mach 8.21 case, using shock unsteadiness $k$-$\omega$ model is compared with the experimental schlieren image in Fig. 4. The shock-shock interaction does not appear to be as clear in experimental schlieren image. A thick boundary layer is formed ahead of the separation shock. The boundary-layer undergoes a compression across the separation shock and bifurcates into two parts. A part of it forms the separated region and part of it flows above separation bubble and further gets compressed across reattachment shock.

The variation of surface properties are shown in Figs. 5 and 6 for both the cases.The baseline $k$-$\omega$ model predicts a delayed initial pressure rise as compared to the experiment and predicts a smaller separation bubble, the new model along with shock unsteadiness $k$-$\omega$ model on the other hand mimics the experimental measurements closely for both cases cases. The pressure plateau between the separation (S) and reattachment (R) points is predicted accurately for Mach 7.18 case, however, it gives a smaller pressure rise at the reattachment location for the strongest Mach 8.21 interaction. The wall pressure drops slightly across the expansion waves after the reattachment region (see Fig. 3) and matches with experiment far downstream.

The wall heat transfer rate computed in the interaction region shows the effect of lower turbulent Prandtl number clearly. The predictions are comparable to the experimental measurements in the reattachment region and in the recovering boundary layer. The heat flux trend inside the separated region also compares well with the experimental data. By comparison, the baseline $k$-$\omega$ model with constant $Pr_T$ overpredicts the peak heat flux by about 50 $\%$ and the trends at the separation point are qualitatively different from that observed in the experiments. The variation of the turbulent Prandtl number based on the shock physics and boundary layer data is thus found to significantly improve the heat flux predictions.

## 4. Conclusion

In this work, we develop a turbulent heat flux model for predicting the wall heat transfer in shock-boundary layer interaction with wall cooling/heating effect. The current model is based on the physics of unsteady shock motion in a turbulent flow, boundary layer DNS data and linear analysis. The model is particularly suitable for high-speed flows with wall cooling. It uses the shock-unsteadiness parameter for flows with upstream vortical and entropic fluctuations typical of hypersonic turbulent boundary layers. The algebraic nature of the new model makes the CFD implementation easier and it can be

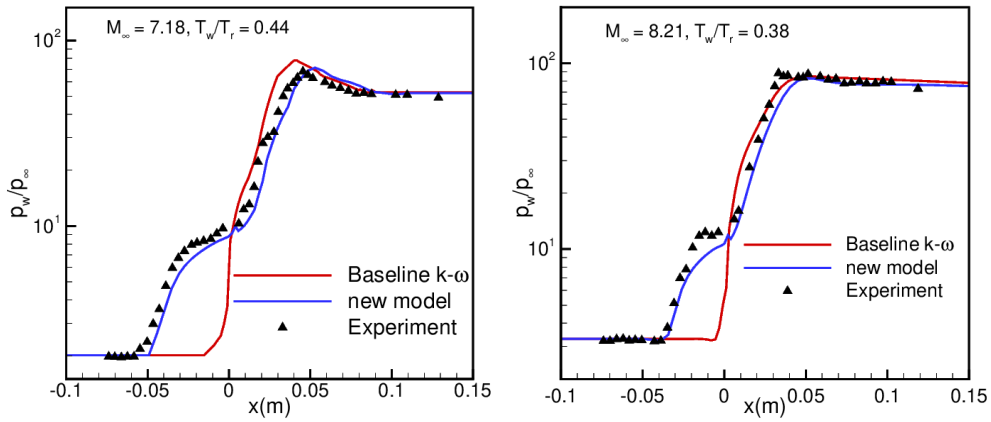


FIGURE 5. Comparison of surface pressure for $M_\infty = 7.18$ and 8.21 respectively, using baseline $k$-$\omega$ and the new variable $Pr_T$ models with the experimental data of Holden [30].

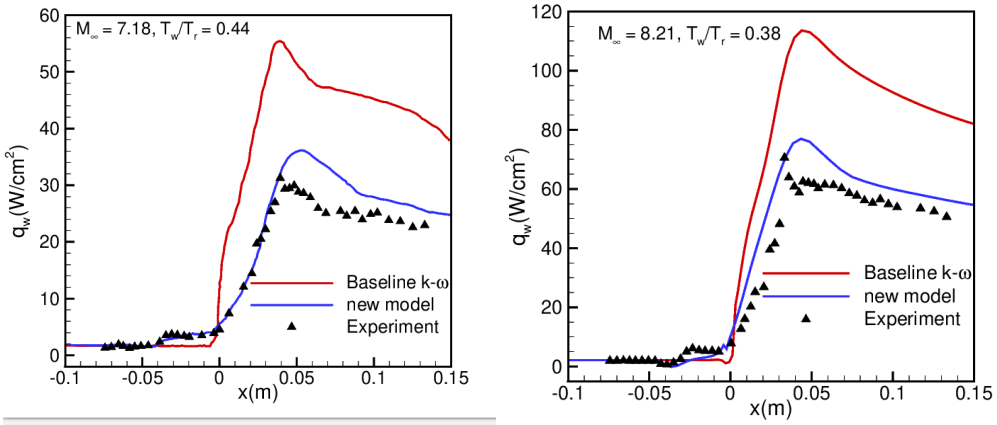


FIGURE 6. Comparison of wall heat flux for $M_\infty = 7.18$ and 8.21 respectively, using baseline $k$-$\omega$ and the new variable $Pr_T$ models with the experimental data of Holden [30].

used with any turbulence model. The new model is then applied to cone-flare geometry at hypersonic Mach numbers with moderate wall cooling and it is found to predict the peak heat transfer consistently well for both the cases. We will apply the model for highly cooled walls ($T_w/T_r$ close to 0.1 – 0.2) in the near future.

## Acknowledgments

Financial support has been provided by the German Research Foundation (Deutsche Forschungsgemeinschaft – DFG) in the framework of the Sonderforschungsbereich Transregio 40. Computational resources have been provided by the Technical University Munich and the LRZ (Leibniz Rechenzentrum).

## References

[1] BOSE, D., BROWN, J.L., PRABHU, D.K., GNOFFO, P., JOHNSTON, C.O. AND HOLLIS, B. (2013). Uncertainty assessment of hypersonic aerothermodynamics

prediction capability. *Journal of Spacecraft and Rockets*, **50**(1), 12–18.

[2] GNOFFO, P.A., BERRY, S.A. AND VAN NORMAN, J.W. (2013). Uncertainty assessments of hypersonic shock wave-turbulent boundary-layer interactions at compression corners. *Journal of Spacecraft and Rockets*, **50**(1), 69–95.

[3] XIAO, X., EDWARDS, J.R., HASSAN, H.A. AND GAFFNEY, R.L. (2007). Role of turbulent prandtl numbers on heat flux at hypersonic mach numbers. *AIAA journal*, **45**(4), 806–813.

[4] OTT, J., KENZAKOWSKI, D. AND DASH, S. (2013). Evaluation of turbulence modeling extensions for the analysis of hypersonic shock wave boundary layer interactions. In: *51st AIAA Aerospace Sciences Meeting Including the New Horizons Forum and Aerospace Exposition*. 983.

[5] ROY, S., PATHAK, U. AND SINHA, K. (2017). Variable turbulent prandtl number model for shock/boundary-layer interaction. *AIAA Journal*, 342–355.

[6] SINHA, K., MAHESH, K. AND CANDLER, G.V. (2003). Modeling shock unsteadiness in shock/turbulence interaction. *Physics of Fluids*, **15**(8), 2290–2297.

[7] QUADROS, R., SINHA, K. AND LARSSON, J. (2016). Turbulent energy flux generated by shock/homogeneous-turbulence interaction. *Journal of Fluid Mechanics*, **796**, 113–157.

[8] SCHÜLEIN, E. (2006). Skin friction and heat flux measurements in shock/boundary layer interaction flows. *AIAA journal*, **44**(8), 1732–1741.

[9] MORKOVIN, M.V. (1962). Effects of compressibility on turbulent flows. *Mécanique de la Turbulence*, **367**, 380.

[10] JAUNET, V., DEBIEVE, J. AND DUPONT, P. (2014). Length scales and time scales of a heated shock-wave/boundary-layer interaction. *AIAA Journal*, **52**(11), 2524–2532.

[11] WAGNER, A., SCHRAMM, J.M., HANNEMANN, K., WHITSIDE, R. AND HICKEY, J.P. (2017). Hypersonic shock wave boundary layer interaction studies on a flat plate at elevated surface temperature. In: *International Conference on RailNewcastle Talks*. Springer, 231–243.

[12] BERNARDINI, M., ASPROULIAS, I., LARSSON, J., PIROZZOLI, S. AND GRASSO, F. (2016). Heat transfer and wall temperature effects in shock wave turbulent boundary layer interactions. *Physical Review Fluids*, **1**(8), 084403.

[13] VOLPIANI, P.S., BERNARDINI, M. AND LARSSON, J. (2018). Effects of a nonadiabatic wall on supersonic shock/boundary-layer interactions. *Physical Review Fluids*, **3**(8), 083401.

[14] VOLPIANI, P.S., WAGNER, A., BERNARDINI, M. AND LARSSON, J. (2019). Using large-eddy simulations to design a new hypersonic shock/boundary-layer interaction experiment. In: *AIAA Scitech 2019 Forum*. 0098.

[15] PIROZZOLI, S., GRASSO, F. AND GATSKI, T. (2004). Direct numerical simulation and analysis of a spatially evolving supersonic turbulent boundary layer at m= 2.25. *Physics of fluids*, **16**(3), 530–545.

[16] DUAN, L., BEEKMAN, I. AND MARTIN, M. (2010). Direct numerical simulation of hypersonic turbulent boundary layers. part 2. effect of wall temperature. *Journal of Fluid Mechanics*, **655**, 419–445.

[17] WILCOX, D.C. (1993). *Turbulence modeling for CFD*. 1 edn. DCW industries La Canada, CA.

[18] VEERA, V.K. AND SINHA, K. (2009). Modeling the effect of upstream temperature fluctuations on shock/homogeneous turbulence interaction. *Physics of fluids*,

**21**(2), 025101.

[19] FORSYTHE, J., HOFFMANN, K. AND DAMEVIN, H.M. (1998). An assessment of several turbulence models for supersonic compression ramp flow. In: *29th AIAA, Fluid Dynamics Conference*. 2648.

[20] COAKLEY, T. AND HUANG, P. (1992). Turbulence modeling for high speed flows. In: *30th Aerospace Sciences Meeting and Exhibit*. 436.

[21] MACCORMACK, R.W. AND CANDLER, G.V. (1989). The solution of the navier-stokes equations using gauss-seidel line relaxation. *Computers & fluids*, **17**(1), 135–150.

[22] SINHA, K. AND CANDLER, G. (1998). Convergence improvement of two-equation turbulence model calculations. In: *29th AIAA, Fluid Dynamics Conference*. 2649.

[23] WRIGHT, M.J., CANDLER, G.V. AND BOSE, D. (1998). Data-parallel line relaxation method for the navier-stokes equations. *AIAA journal*, **36**(9), 1603–1609.

[24] MENTER, F.R. (1994). Two-equation eddy-viscosity turbulence models for engineering applications. *AIAA journal*, **32**(8), 1598–1605.

[25] ROY, S. AND SINHA, K. (2018). Variable turbulent prandtl number model applied to hypersonic shock/boundary-layer interactions. In: *2018 Fluid Dynamics Conference*. 3728.

[26] ROY, S. AND SINHA, K. (2019). Turbulent heat flux model for hypersonic shock–boundary layer interaction. *AIAA Journal*, 1–6.

[27] WALZ, A. (1969). *Boundary layers of flow and temperature*. MIT press.

[28] LESCHZINER, M., BATTEN, P. AND LOYAU, H. (2000). Modelling shock-affected near-wall flows with anisotropy-resolving turbulence closures. *International Journal of Heat and Fluid Flow*, **21**(3), 239–251.

[29] HUANG, P., COLEMAN, G. AND BRADSHAW, P. (1995). Compressible turbulent channel flows: Dns results and modelling. *Journal of Fluid Mechanics*, **305**, 185–218.

[30] HOLDEN, M.S., WADHAMS, T.P. AND MACLEAN, M.G. (2013). Measurements in regions of shock wave/turbulent boundary layer interaction from mach 4 to 10 for open and "blind" code evaluation/validation. In: *21st AIAA Computational Fluid Dynamics Conference*. 2836.

[31] PASHA, A.A. AND SINHA, K. (2012). Simulation of hypersonic shock/turbulent boundary-layer interactions using shock-unsteadiness model. *Journal of Propulsion and Power*, **28**(1), 46–60.